J Appl Electrochem (2014) 44:255–261
DOI 10.1007/s10800-013-0652-0

RESEARCH ARTICLE

A study of Mo-modified Pd/MWCNT catalysts for ethanol oxidation in the alkaline solution

Weimin Chen · Yu Zhang

Received: 23 August 2013 / Accepted: 2 December 2013 / Published online: 12 December 2013

Abstract The effect of the modification of Pd-based electrocatalysts by molybdenum on the catalytic performance toward ethanol oxidation in the alkaline solution is investigated. The results indicate that the molybdenum oxide/hydroxide assists in the uniform distribution of Pd nanoparticles on the surface of the carbon support. The catalytic performance of the Mo-modified Pd/MWCNT catalyst is largely dependent on the temperature at which the molybdenum oxide/hydroxide is heat-treated. The catalyst prepared from the molybdenum oxide/hydroxide heat-treated at 350 °C has the highest catalytic activity and the best poison resistance. X-ray photoelectron spectroscopy results reveal that there is an interaction between Pd and Mo in Mo-modified Pd/MWCNT catalysts. The moderately dehydrated and oxidized molybdenum oxide/hydroxide has the strongest effect on promoting the catalytic activity and the poison resistance of Pd-based nanocatalysts for ethanol oxidation.

Keywords Electrocatalyst · Ethanol oxidation · Palladium · Molybdenum

1 Introduction

Alkaline direct alcohol fuel cells (ADAFCs) attract increasing attentions recently due to their good performances and low costs. In acidic media, the expensive Pt-based nanocatalysts are widely used as the alcohol-oxidation catalysts; while in alkaline media, the oxidation of alcohols can be readily catalyzed by the less-expensive Pd-based nanocatalysts [1–3]. In addition, some non-noble metals that serve as promoters such as Ni and Co are electrochemically stable in alkaline environments. For those reasons, enormous efforts have been devoted to develop high-performance Pd-based nanocatalysts for alcohol oxidation in alkaline media. The addition of transition metals is thought to be a useful means of improving the catalytic activity and the poison resistance of fuel cell catalysts. It has been reported that several transition metals, such as Ni [4–8], Au [9–12], Bi [13, 14], Rh [15], Pb [16], and In [17], exhibit promoting effects on the electrooxidation of ethanol in alkaline media.

Molybdenum is widely used to modify electrocatalysts for alcohol-oxidation in acidic media due to its characteristics such as multiple valences, excellent redox character, and mixed conductivities [18–24]. But research works about the modification of Pd-based catalysts by molybdenum for ethanol oxidation in alkaline media has rarely been reported. In this work, Mo-modified multiwalled carbon nanotube (MWCNT) supported Pd-based catalysts were prepared by an ethylene glycol reduction method, and their catalytic performances for ethanol oxidation were evaluated. Considering the dependence of the chemical properties of the molybdenum oxides/hydroxides on the heat-treating temperature, Pd-based nanocatalysts were modified by molybdenum oxides/hydroxides heat-treated at the temperatures of 150, 350, and 400 °C, respectively. The catalytic performances of Mo-modified Pd-based catalysts for ethanol oxidation were examined.

2 Experimental

2.1 Preparation

The Pd/MWCNT nanocatalyst was prepared using an ethylene glycol (EG) reduction method [25]. Typically,

W. Chen (✉) · Y. Zhang
School of Environmental and Chemical Engineering, Shenyang Ligong University, Shenyang 110159, China
e-mail: cwmchem@163.com

160 mg of treated MWCNT (purchased form Chengdu Organic Chemicals Co. Ltd., and treated with 6 mol L^{-1} H_2SO_4–HNO_3 solution at 110 °C for 2 h) was suspended in an appropriate amount of EG solution under vigorous agitation. Then 16.8 mL of the EG solution (2.38 mg Pd mL^{-1}) of palladium chloride (Sinopharm Chemical Reagent Co. Ltd.) was added into the suspension dropwise. The pH value of the suspension was adjusted to about 10 by adding 1 mol L^{-1} sodium hydroxide solution. The mixture was refluxed in an oil bath at 130 °C for 2.5 h. Afterward, the mixture was filtered and washed with deionized water, and then dried at 70 °C in a vacuum oven for 12 h. For Mo-modified Pd/MWCNT catalysts, before the reduction of the Pd precursor, the treated MWCNT was deposited with the molybdenum oxide/hydroxide by adding ammonium molybdate and sodium borohydride into the suspension under a vigorous agitation and adjusting the pH value to about 1. The modified MWCNT was filtered and heat-treated in the air at the temperatures of 150, 350, and 400 °C, respectively. The molar ratio of Pd to Mo in Mo-modified Pd/MWCNT catalysts was 1:0.2.

2.2 Characterization

Transmission electron microscopy (TEM) measurements were carried out using a JEOL JEM-2000EX microscope operating at 120 kV. The size distribution and the mean particle size of the electrocatalysts were obtained by measuring more than 200 particles from TEM images. X-ray photoelectron spectra (XPS) were collected on a Thermo VG ESCALAB250 multifunction surface analysis system with a monochromatic aluminum Kα (1,486.6 eV) X-ray source operating at 150 W. The differential thermal analysis (DTA) measurement was conducted using a DTA-100 differential thermal analyzer (Beijing Henven Scientific Instrument).

Electrochemical measurements were carried out at 25 °C, using a three-electrode system. The working electrode was a glassy carbon electrode with a diameter of 4 mm. The counter electrode was a Pt-foil and the reference electrode was a saturated calomel electrode (SCE). Catalyst inks were made by mixing 5 mg of the catalyst with 50 µL of 5 wt% Nafion® ionomer solution (EW = 1,100, DuPont Corp.) and 1 mL of ethanol ultrasonically for 30 min. In electrode preparation, 25 µL of the prepared catalyst slurry was pipetted onto the glassy carbon electrode, and the solvent was evaporated. Electrochemical measurements were conducted using a PAR2273 potentiostat/galvanostat. The scan rate of the cyclic voltammetry (CV) measurement and the linear sweep voltammetry (LSV) measurement were 20 and 1 mV s^{-1}, respectively. For the electrochemical impedance spectroscopy (EIS) measurement, impedance spectra were recorded at five points per decade by superimposing a 5 mV ac signal on the cell under potentiostatic mode over the frequency range from 100 kHz to 0.1 Hz. The applied potential value was −0.25 V versus SCE.

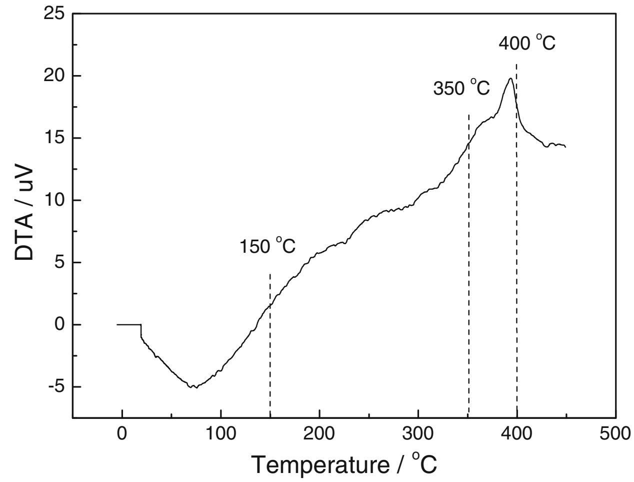

Fig. 1 The DTA curve of the as-prepared molybdenum oxide/hydroxide

3 Results and discussion

The DTA curve of the as-prepared molybdenum oxide/hydroxide is shown in Fig. 1. It is seen that there is a wide endothermic peak within the temperature range of 25–130 °C, corresponding to the removal of the hygroscopic water. It is also seen that several weak endothermic peaks appear within the temperature range of 220–330 °C, which can be assigned to the removal of structural hydroxyls. This temperature range corresponds to a moderate dehydration and oxidation of the Mo compounds. As the temperature exceeds 392 °C, a drastic endothermic reaction begins to take place, implying a deep dehydration and oxidation of the molybdenum oxide/hydroxide. This result suggests that with the increase in the heat-treating temperature, the molybdenum oxide/hydroxide is dehydrated and oxidized gradually, and finally, they are converted to high-valence oxides such as MoO_3. Based on this result, in our experiment, heat-treating temperatures of 150, 350, and 400 °C are selected to represent the temperatures at which the Mo compounds undergo light, moderate, and deep dehydration/oxidation, respectively. In this way, the prepared Mo-modified Pd-based catalysts are denoted as PdMo/MWCNT150, PdMo/MWCNT350, and PdMo/MWCNT400, respectively.

The cyclic voltammetry curves of catalysts recorded in 1.0 mol L^{-1} C_2H_5OH–1.0 mol L^{-1} KOH solution are shown in Fig. 2. It is seen that the ethanol-oxidation peaks in the forward scan in PdMo/MWCNT150 and

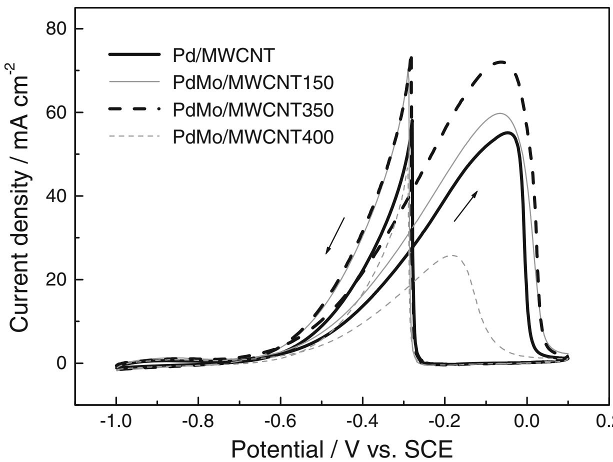

Fig. 2 CV curves of catalysts recorded in 1.0 mol L^{-1} C_2H_5OH–1.0 mol L^{-1} KOH solution. Scan rate 20 mV s^{-1}

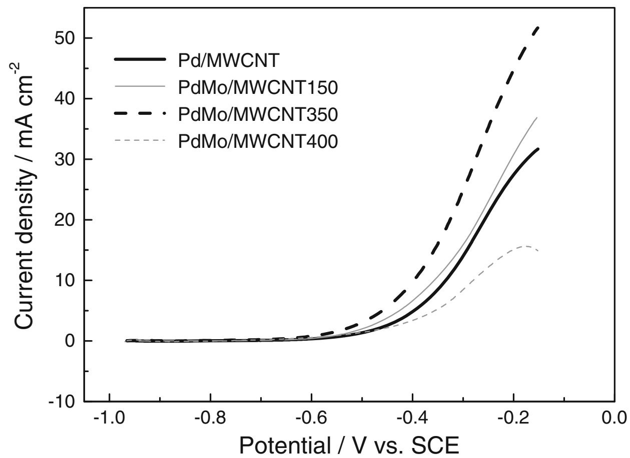

Fig. 3 LSV curves of catalysts recorded in 1.0 mol L^{-1} C_2H_5OH–1.0 mol L^{-1} KOH solution. Scan rate 1 mV s^{-1}

PdMo/MWCNT350 are higher than that in Pd/MWCNT, but in PdMo/MWCNT400, the peak is relatively low. PdMo/MWCNT350 has the highest catalytic activity. This result suggests that the moderately dehydrated and oxidized Mo compound has the strongest effect on promoting the catalytic performance of the Pd-based catalyst, while the deeply dehydrated and oxidized Mo compound is detrimental to the Pd-based catalyst. The mechanism of ethanol oxidation on Pd-based catalysts can be expressed by Eqs. 1–3.

$$\mathrm{Pd} + \mathrm{OH}^- \rightarrow \mathrm{Pd{-}OH_{ads}} + \mathrm{e}^- \tag{1}$$

$$\mathrm{Pd{-}(CH_3CH_2OH)_{ads}} + 3\mathrm{OH}^- \rightarrow \mathrm{Pd{-}(COCH_3)_{ads}} + 3\mathrm{H_2O} + 3\mathrm{e}^- \tag{2}$$

$$\mathrm{Pd{-}(COCH_3)_{ads}} + \mathrm{Pd{-}OH_{ads}} \rightarrow \mathrm{Pd{-}CH_3COOH} + \mathrm{Pd} \tag{3}$$

It is suggested that the removal of the adsorbed acyl by the adsorbed hydroxyl (Eq. 3) is the rate-determining step. Thus, the relatively high catalytic activities of PdMo/MWCNT150 and PdMo/MWCNT350 may be largely attributed to the high surface contents of adsorbed hydroxyl due to the existence of the molybdenum oxide/hydroxide. This assumption is supported by the XPS results presented in the following texts. It is also seen from Fig. 2 that the ethanol-oxidation peaks in PdMo/MWCNT150 and PdMo/MWCNT350 are wider than that in Pd/MWCNT. This result indicates that the oxidation of ethanol occurs within a wider potential region in PdMo/MWCNT150 and PdMo/MWCNT350, implying that there are different kinds of active sites on the catalyst surfaces.

Figure 3 shows the linear sweep voltammetry curves of catalysts recorded in 1.0 mol L^{-1} C_2H_5OH–1.0 mol L^{-1} KOH solution. The onset potentials for ethanol oxidation in PdMo/MWCNT150 and PdMo/MWCNT350 are −0.537 and −0.582 V, respectively, lower than that in Pd/MWCNT

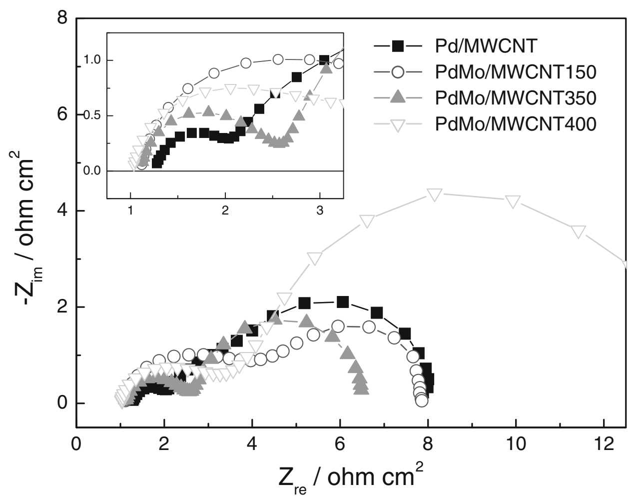

Fig. 4 EIS spectra of catalysts in 1.0 mol L^{-1} C_2H_5OH–1.0 mol L^{-1} KOH solution

(−0.518 V). PdMo/MWCNT350 has the lowest onset potential. This result implies that in PdMo/MWCNT150 and PdMo/MWCNT350, the existence of the molybdenum oxide/hydroxide leads to a low active energy and an improved dynamics for ethanol oxidation. In contrast, PdMo/MWCNT400 exhibits a poor ethanol-oxidation dynamics, which is consistent with the CV results (Fig. 2).

The EIS results of catalysts in 1.0 mol L^{-1} C_2H_5OH–1.0 mol L^{-1} KOH solution are shown in Fig. 4. The Nyquist diagram consists of two arcs. The small arc that appears at the high frequency range relates to electrical conduction via the electrical double layer or via geometric boundaries [26]. The arc that appears at the low frequency range relates to the electro-oxidation of ethanol [27]. Obviously, PdMo/MWCNT350 has the smallest charge transfer resistance, implying a high ethanol-oxidation activity. It is also observed from the inset of Fig. 4 that the

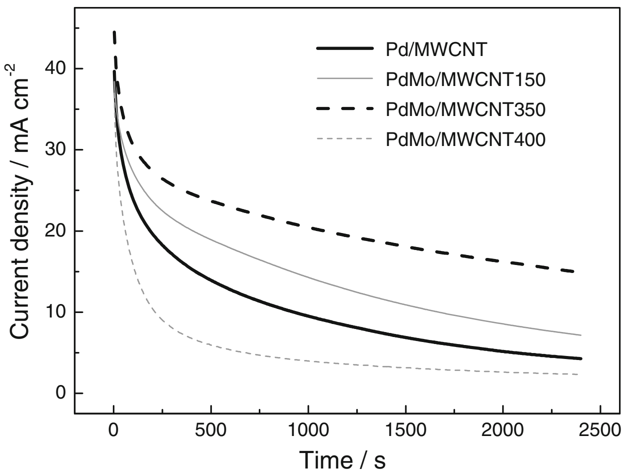

Fig. 5 CA curves of catalysts recorded in 1.0 mol L^{-1} C_2H_5OH–1.0 mol L^{-1} KOH solution

ohmic resistances (the intersection of the higher frequency arc on the real axis) in Mo-modified catalysts are lower than that in Pd/MWCNT, which could be explained by the mixed electron/proton conductivity in molybdenum oxides/hydroxides [21, 22].

Figure 5 shows the chronoamperometry (CA) curves of catalysts recorded in 1.0 mol L^{-1} C_2H_5OH–1.0 mol L^{-1} KOH solution. By measuring the current densities at different times during the test, the performance losses can be calculated. The results show that within the time span of 10–2,400 s, the performance losses in Pd/MWCNT, PdMo/MWCNT150, PdMo/MWCNT350, and PdMo/MWCNT400 are 88.2, 80.2, 63.8, and 92.7 %, respectively. Because the performance losses of catalysts are mainly caused by the accumulation of intermediates such as $(CH_3CHO)_{ads}$ on the active sites, this result indicates that PdMo/MWCNT350 has the highest poison resistance.

The TEM images of catalysts are shown in Fig. 6. The mean particle sizes of Pd/MWCNT, PdMo/MWCNT150, PdMo/MWCNT350, and PdMo/MWCNT400 are measured to be 2.0, 2.2, 2.2, and 2.3 nm, respectively. Pd/MWCNT has a relatively small mean particle size, but there is some degree of agglomeration. Mo-modified catalysts exhibit uniform distributions of Pd nanoparticles on the MWCNT,

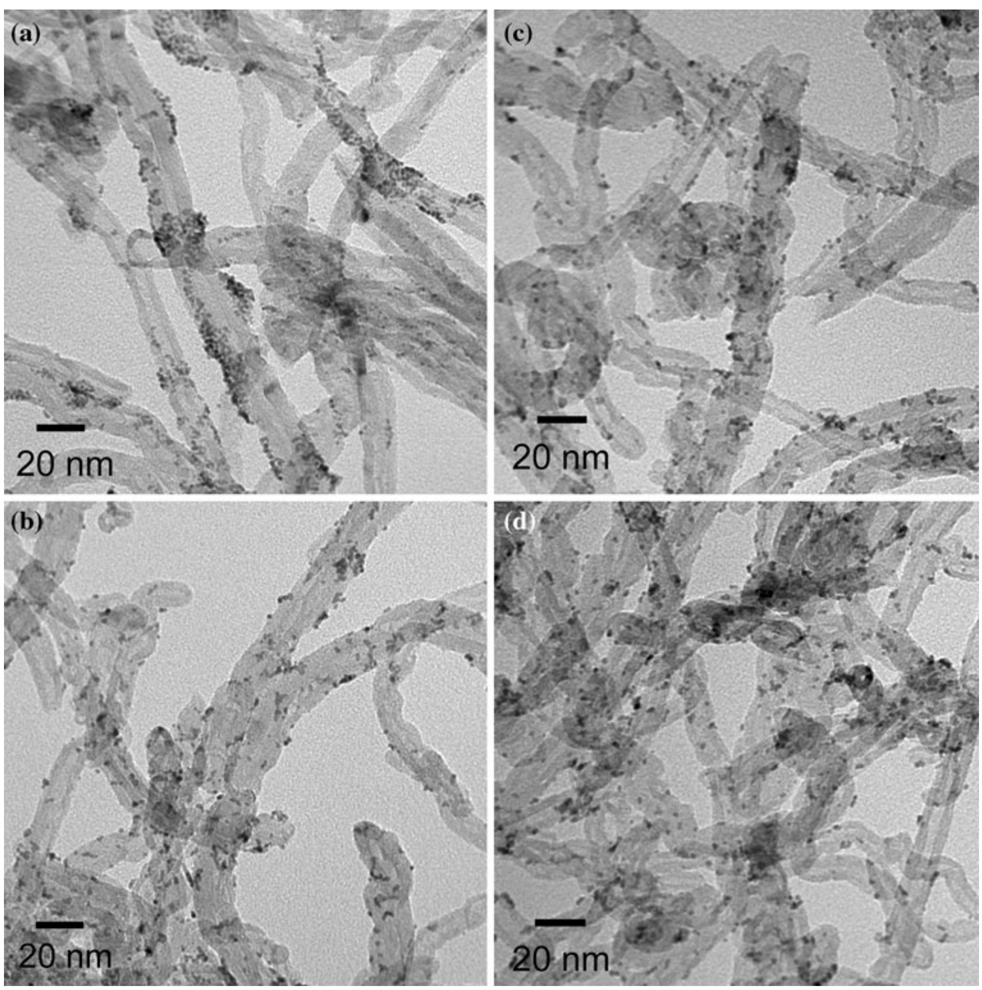

Fig. 6 TEM images of catalysts: **a** Pd/MWCNT; **b** PdMo/MWCNT150; **c** PdMo/MWCNT350; **d** PdMo/MWCNT400

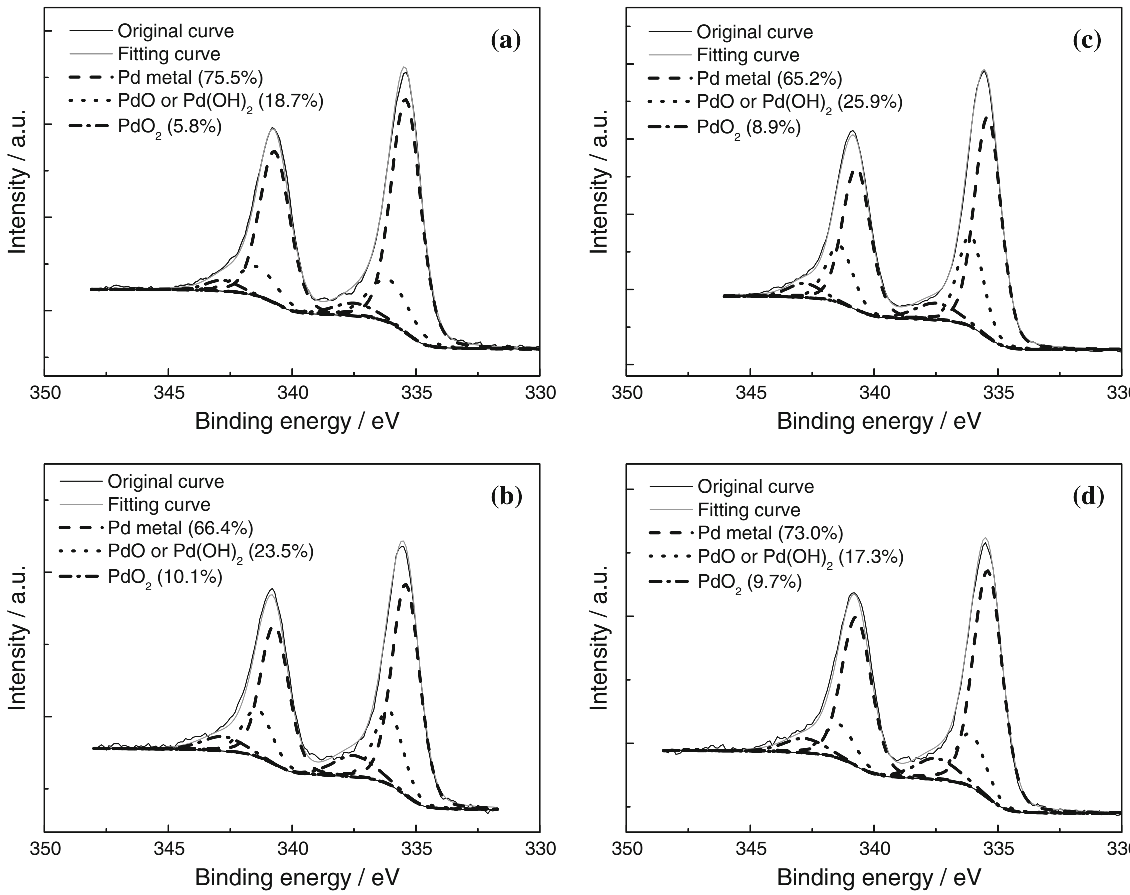

Fig. 7 Pd 3d region of XPS spectra of catalyst samples: **a** Pd/MWCNT; **b** PdMo/MWCNT150; **c** PdMo/MWCNT350; **d** PdMo/MWCNT400

which could be largely ascribed to the interaction between the Pd precursor and the molybdenum oxide/hydroxide during the preparation.

The Pd 3d XPS spectra of catalysts are shown in Fig. 7. Pd exists in different chemical states in the catalysts. The doublet appears at the binding energies of 335.4 and 340.7 eV is attributed to metallic palladium Pd(0). The doublet appears at the binding energies of 336.1 and 341.4 eV is assigned to Pd(II) species such as PdO and $Pd(OH)_2$. The doublet appears at the binding energies of 337.5 and 342.8 eV could be assigned to Pd species in a higher chemical state such as PdO_2 and other Pd(IV) species adsorbed on the metal surface. The deconvolution results of the Pd $3d_{5/2}$ XPS spectra show that the Pd(0) contents in PdMo/MWCNT150, PdMo/MWCNT350, and PdMo/MWCNT400 are 66.4, 65.2, and 73.0 %, respectively, lower than that in Pd/MWCNT (75.5 %). This result suggests that there is an interaction between Pd and Mo. The remarkably lower Pd(0) contents in PdMo/MWCNT150 and PdMo/MWCNT350 than in Pd/MWCNT imply that the interaction is much stronger in PdMo/MWCNT150 and PdMo/MWCNT350 than in PdMo/MWCNT400.

The O 1s XPS spectra of catalysts are shown in Fig. 8. It is seen that the O 1s spectra are composed of two O species, i.e., the O species in noble/transition metal oxides (531.0 eV) and the O species in hydroxides (532.8 eV). The curve-fitting results show that the contents of hydroxides in PdMo/MWCNT150, PdMo/MWCNT350, and PdMo/MWCNT400 are 83.2, 74.9, and 66.9 %, respectively, much higher than that in Pd/MWCNT (59.6 %). This result indicates that the introduction of molybdenum brings a large amount of hydroxides onto the catalyst surface, and after the heat treatment, parts of those hydroxides were dehydrated and converted to oxides. The high catalytic performance of PdMo/MWCNT350 likely suggests that the Mo-modified Pd/MWCNT with an approximately 75 % surface content of hydroxides has the highest catalytic activity and the best poison resistance.

The Mo 3d XPS spectra of catalysts are shown in Fig. 9. It is observed that with the increase in the heat-treating temperature, the Mo $3d_{5/2}$ peak tends to shift toward higher binding energies. This phenomenon indicates that with the increase in the heat-treating temperature, the molybdenum oxide/hydroxide was dehydrated and oxidized gradually. The high catalytic performance of PdMo/MWCNT350

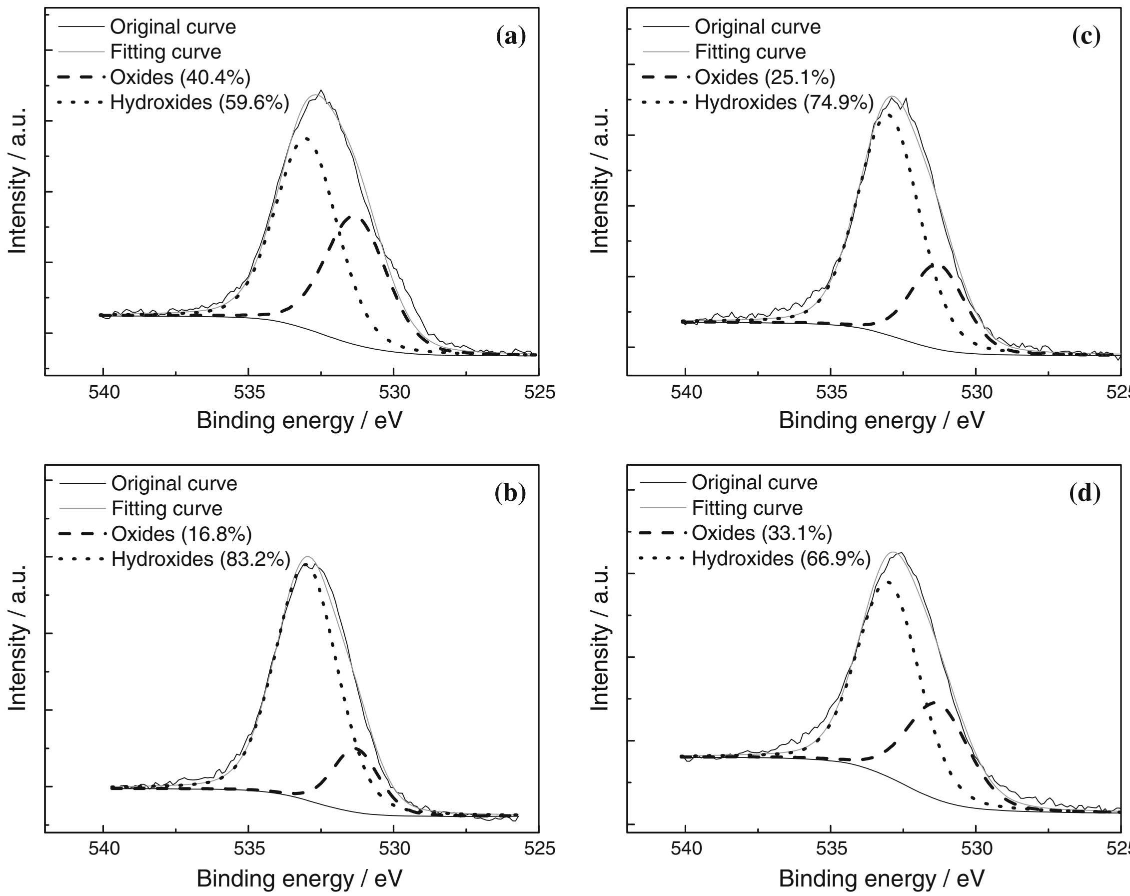

Fig. 8 O 1s region of XPS spectra of catalyst samples: **a** Pd/MWCNT; **b** PdMo/MWCNT150; **c** PdMo/MWCNT350; **d** PdMo/MWCNT400

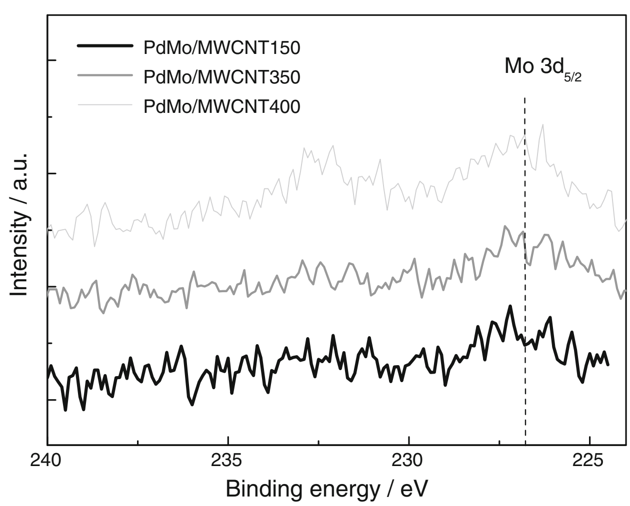

Fig. 9 Mo 3d region of XPS spectra of catalyst samples: **a** Pd/MWCNT; **b** PdMo/MWCNT150; **c** PdMo/MWCNT350; **d** PdMo/MWCNT400

suggests that the moderately dehydrated and oxidized molybdenum oxide/hydroxide has the strongest effect on promoting the catalytic performance of Pd/MWCNT toward ethanol oxidation. It has been reported that the molybdenum oxide/hydroxide with a mixed Mo valence has promoting effects on the oxidation of methanol and ethanol in acidic media. MoO_x promotes the water activation and facilitate the oxidation of intermediate species [19, 24]. The result of this work suggests that in alkaline media, the mixed-valence molybdenum oxide/hydroxide also has a remarkable promoting effect on the electrooxidation of ethanol.

4 Conclusions

The Mo-modification has a remarkable influence on the catalytic performance of Pd-based nanocatalysts toward ethanol oxidation in the alkaline solution. The molybdenum oxide/hydroxide assists in the uniform distribution of Pd nanoparticles on the surface of the carbon support. There is an interaction between Pd and Mo in Mo-modified Pd-based catalysts. The effect of the Mo-modification on the catalytic performance of Pd-based catalysts is dependant on the extent of the dehydration and the oxidation of the molybdenum oxide/hydroxide. The moderately dehydrated and oxidized molybdenum oxide/hydroxide has the

strongest effect on promoting the catalytic activity and the poison resistance of Pd-based nanocatalysts for ethanol oxidation.

Acknowledgments This work was financially supported by the National Natural Science Foundation of China (Grant No. 21273152).

References

1. Bianchini C, Shen PK (2009) Chem Rev 109:4183–4206
2. Brouzgou A, Song SQ, Tsiakaras P (2012) Appl Catal B 127:371–388
3. Brouzgou A, Podias A, Tsiakaras P (2013) J Appl Electrochem 43(2):119–136
4. Su PC, Chen HS, Chen TY et al (2013) Int J Hydrogen Energy 38(11):4474–4482
5. Qi Z, Geng H, Wang X et al (2011) J Power Sources 196:5823–5828
6. Wei YC, Liu CW, Kang WD et al (2011) J Electroanal Chem 660:64–70
7. Zhang M, Yan Z, Xie J (2012) Electrochim Acta 77:237–243
8. Shen SY, Zhao TS, Xu JB et al (2010) J Power Sources 195:1001–1006
9. Feng YY, Liu ZH, Xu Y et al (2013) J Power Sources 232:99–105
10. Li F, Guo Y, Li R et al (2013) J Mater Chem A 1:6579–6587
11. Song HM, Anjum DH, Sougrat R et al (2012) J Mater Chem 22:25003–25010
12. Lee YW, Kim M, Kim Y et al (2010) J Phys Chem C 114:7689–7693
13. Cai J, Huang Y, Guo Y (2013) Electrochim Acta 99:22–29
14. Neto AO, Tusi MM, Polanco NSD et al (2011) Int J Hydrogen Energy 36:10522–10526
15. Shen S, Zhao T (2013) J Mater Chem A 1:906–912
16. Wang Y, Nguyen TS, Liu X et al (2010) J Power Sources 195:2619–2622
17. Chu D, Wang J, Wang S et al (2009) Catal Commun 10:955–958
18. Cui ZM, Jiang SP, Li CM (2011) Chem Commun 47:8418–8420
19. Lee E, Murthy A, Manthiram A (2011) Electrochim Acta 56:1611–1618
20. García G, Tsiouvaras N, Pastor E et al (2012) Int J Hydrogen Energy 37:7131–7140
21. Justin P, Ranga Rao G (2011) Int J Hydrogen Energy 36:5875–5884
22. Ma L, Zhao X, Si F et al (2010) Electrochim Acta 55:9105–9112
23. Xiang XD, Huang QM, Fu Z et al (2012) Int J Hydrogen Energy 37:4710–4716
24. Martínez-Huerta MV, Tsiouvaras N, Peña MA et al (2010) Electrochim Acta 55:7634–7642
25. Zhou Z, Wang S, Zhou W et al (2003) Chem Commun 3:394–395
26. Otomo J, Li X, Kobayashi T et al (2004) J Electroanal Chem 573:99–109
27. Hsing IM, Wang X, Leng YJ (2002) J Electrochem Soc 149(5):A615–A621